Durable Flexible Supercapacitors Utilizing the Multifunctional Role of Ionic Liquid

DOI: 10.1002/ ((please add manuscript number))
Article type: (Full Paper)

Durable Flexible Supercapacitors Using Multifunctional Role of Ionic Liquids

*Marta Lorenzo and Geetha Srinivasan**

Ms. M. Lorenzo, Dr G. Srinivasan
School of Chemistry and Chemical Engineering, The QUILL Research Centre, David Keir Building, Queen's University Belfast, Stranmillis Road Belfast BT9 5AG, UK
g.srinivasan@qub.ac.uk

Keywords: conducting polymers, ionic liquids, supercapacitors, flexible devices, energy storage medical device

Abstract

A simple scalable approach to design flexible, ultrathin and safe supercapacitors to power-up the next-generation portable electronics and implantable biomedical devices is reported. The main challenge to construct flexible supercapacitors is the development of flexible electrodes that can retain characteristics of high power density, long cycle life and high efficiency during and after bending conditions. In the current work, flexible electrodes based on conducting polymer-biopolymer-ionic liquid-graphite composites that are chemically blended and stable have been prepared to utilize as electrodes in the fabrication of three devices viz. (i) electrochemical, (ii) electrical double-layer and (iii) hybrid supercapacitors. The multifunctional role of ionic liquids as solvent, electrolyte and plasticizer has been exploited to fabricate these novel supercapacitors. These flexible supercapacitors show specific capacitance values around 5 mF g^{-1}, operational voltage of ~2.2 V and an excellent cycle life of >15000 cycles with nearly 100% efficiency. The designer nature of these electrodes, chemical stability and feasibility to use biocompatible components will enable the construction of task specific supercapacitors with excellent device stability.

1. Introduction

With the boom in technology over the last decades, need for smart materials that can function on external activation for use in modern electronic devices has increased tremendously. According to a survey by Market Research Store,[1] Global Market Outlook for smart materials cost was accounted to $34.3 billion and expected to raise to $80.2 billion by 2020. On the other hand, Environmental Protection Agency reported 3,140,000 tons of electronic waste was generated in 2013 and is urging to use bio-renewable sources for electronic materials fabrication.[2] Considering the two ends of the research impact, there is a growing need for developing electronic materials from natural resources such as bio-waste, specifically for energy storage device applications. Supercapacitors[3] are promising modern energy storage systems owing to their high specific power, long cyclability when compared to rechargeable batteries, fast charging, environmentally friendly, and safe nature.[4] Recently there is a growing demand for flexible supercapacitors in wearable electronics.[5] Conducting polymers (CPs)[6] are researched widely for flexible supercapacitor applications in the literature.[7] CPs are organic polymers that exhibit electrical, magnetic and optical properties usually associated with metals, whilst also retaining many advantageous mechanical properties of a polymer. CPs are classified as 'smart materials' due to their inherent property to accept a counter ion for charge balance when oxidized and to expel the counter ion when reduced. However, CPs suffer from a number of disadvantages: they are intractable, insoluble and not thermoformable. Therefore, their processability is a challenge and restricts their direct usage in real life applications wherein flexibility is a requirement. Alternatively, CPs can be made flexible by grafting them on paper,[8] fabric[9] or by modifying carbon electrodes such as graphene.[10] However grafted polymers suffer from poor adherence to the surface of their host materials and inhomogeneity leading to non-uniform active surfaces. Therefore, supercapacitors based on CPs face problems such as capacitance fade, incomplete electro-

wetting, restrictions in the thickness of electrodes, mechanical stability, and usage of environmentally toxic chemicals. On the other hand, metallic semiconducting free-standing flexible films are experimentally challenging and expensive to prepare on a large scale.

Recently we demonstrated the fabrication of a new class of electro-active materials that are inherently homogeneous and flexible, however retaining the smart functionality of the CPs using ionic liquids (ILs) technology.[11] Our flexible conducting polymer–biopolymer-ionic liquid composites[11] constitute more durable electrodes; ionic liquids are safe replacements for organic solvent/aqueous based electrolytes as they impart longer cycle life, are non-flammable, could be incorporated into biopolymer membranes such as cellulose to provide solid-state electrolytes with no leakage issues and possess lower internal resistance. On the other hand, ILs have been identified as safe electrolyte candidates for electrochemical device applications due to their superior qualities including good conductivity, wide electrochemical window (EW), non-flammable nature and negligible vapor pressure characteristics.[12] Flexible energy devices are not only advantageous in portable electronic devices that are used in our daily life, such as laptops, smartphones and tablets but also have great potential in biomedical applications for supplying power for health monitoring and treatment purposes.[13] Currently, a primary battery such as a lithium battery is used to power the medical devices.[14] Usage of harmful organic solvents, electrolyte leakage, potential explosion, and high internal resistance are the hazards associated with using lithium batteries to power the medical implants. These rigid energy devices are also implanted under the skin which is wired to the medical device and this causes patient discomfort to adapt their body shapes to fit these rigid batteries. Replacement of lithium batteries with flexible supercapacitors composed of biocompatible organic composites and green electrolytes would, therefore, be highly advantageous for biomedical applications.[15] Development of supercapacitors using electronically conducting polymer composites utilizing a biopolymer

available in bio-waste to provide a flexible matrix, using an ionic liquid technology is the cynosure of this work. CPs provide the smart functionality in these composites and ionic liquids increase the electro-activity and plasticity leading to more durable supercapacitors with the flexible nature to adapt to body shapes.

General preparation of conducting polymer-biopolymer-ionic liquid composite was carried out using the procedure reported earlier.[11] Polypyrrole (PPy) was used as the conducting polymer, cellulose (Cell) as the biopolymer and trihexyl(tetradecyl)phosphonium bis{(trifluoromethyl)sulfonyl} amide, $[P_{6,6,6,14}][NTf_2]$, (IL) as the ionic liquid plasticizer to form PPy-Cell-IL composite film. Cellulose regeneration process using ionic liquids was exploited to make these materials.[16] Due to in situ preparation of PPy with hydrogen bonding to cellulose in the solution state using 1-butyl-3-methylimidazolium chloride ($[C_4mim]Cl$) ionic liquid as the solvent, the PPy-Cell-IL composite films prepared by this method were inherently homogeneous and flexible. Graphite was added to improve conductivity to form PPy-Cell-IL-Graphite composite film. Graphite was dispersed in cellulose matrix to form Graphite-Cell-IL composite films. 10 wt% of $[P_{6,6,6,14}][NTf_2]$ IL was incorporated in all composites to induce plasticity[17] and also to facilitate electro-wetting during device performance. This IL plasticizer was also chosen to be biocompatible as reported earlier.[11, 18] The average thickness of these composite films when dried was ~50 μm. The fabrication of the symmetrical supercapacitor was carried out by punch-cutting 1 cm^2 size sheets of the composite films described above, sandwiched with a 1.5 cm^2 paper separator dip coated with 1-ethyl-3-methylimidazolium bis{(trifluoromethyl)sulfonyl}amide ($[C_2mim][NTf_2]$) ionic liquid as shown in **Figure 1**. Conventional kitchen aluminum foils were used as current collectors and waterproof polyester self-adhesive sheets were used for packaging. Total device thickness of these supercapacitors (excluding current collectors)

were around ~150 µm leading to an ultrathin flexible assembly that can be suitable for medical implant applications.[19]

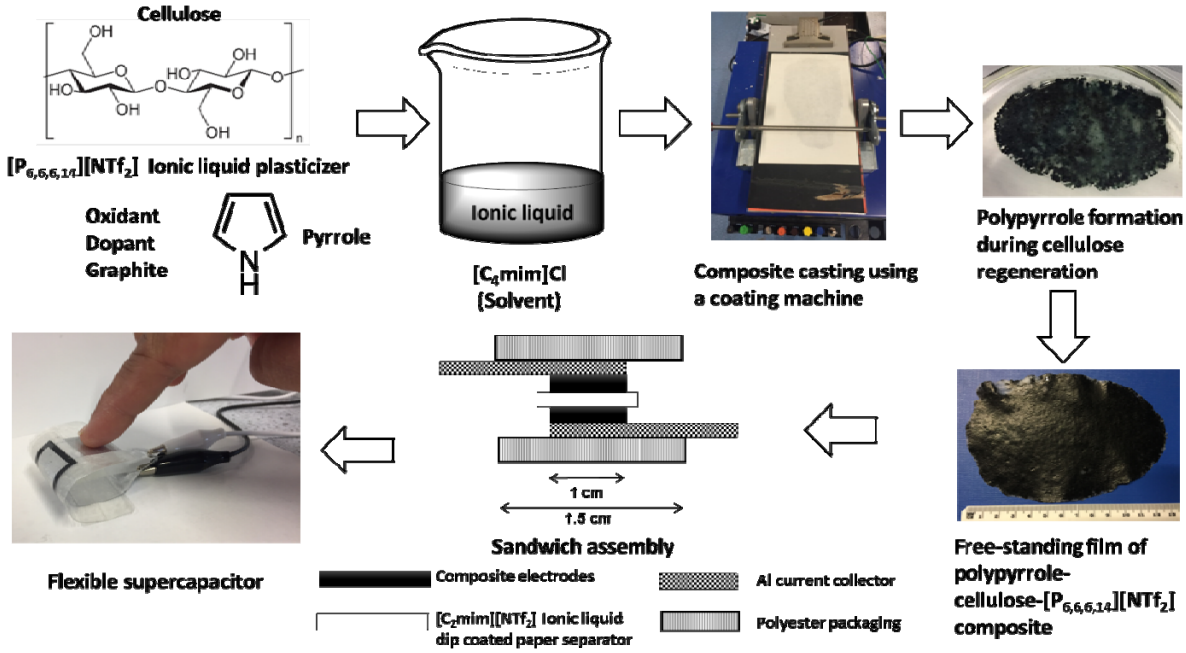

Figure 1. Schematic of the fabrication process of polypyrrole-cellulose-ionic liquid composite films leading to flexible supercapacitors.

2. Results and Discussion

2.1. Electrochemical characterization

To understand the charge storage and release mechanism from these new materials, three types of energy devices were fabricated: (a) electrochemical supercapacitor (ES),[7a] (b) electrical double-layer supercapacitor (EDLS),[20] and (c) hybrid supercapacitor (HS).[21] An electrochemical supercapacitor (also known as pseudocapacitor)[3] follows a redox mechanism for the charge storage and release process, an electrical double-layer supercapacitor depends on the electrostatic forces forming a double-layer at the electrode-electrolyte interface and the hybrid supercapacitor possesses both electrochemical and electrical process for the energy storage and release mechanism. PPy-Cell-IL composite film was used as electrodes to fabricate the ES exploiting the redox-active nature of PPy,

Graphite-Cell-IL film was used to fabricate EDLS wherein the electrical double-layer formation is influenced by graphite and PPy-Cell-IL-Graphite composite film was used for HS assembly, as it contains both PPy and graphite to contribute to electrochemical and electrical double-layer charge storage and release mechanism, respectively.

To evaluate the electrochemical properties of the newly developed cellulose composites in the three types of energy devices (ES, EDLS, and HS), the $[C_2mim][NTf_2]$ IL electrolyte was kept constant in order to eliminate the variation in device performance influenced by the electrolyte-electrode interaction when using different electrolytes. Electrochemical behavior of the fabricated supercapacitors was examined using cyclic voltammetry (CV), galvanostatic charge-discharge studies (GCD), and electrical impedance spectroscopy (EIS). The nearly rectangular shaped and symmetric voltammograms[3] for all the devices even at a higher scan rate of 1V sec^{-1} was retained. ES, EDLS and HS device voltammograms at the scan rate of 50 mV sec^{-1} presented in **Figure 2**a (all scan rates are shown in supporting information (SI) Figure S1, S5 and S9) showed the capacitive behavior of these energy storage devices. The electrochemical window (working potential) of these devices vary between 1.6 V to 2.2 V comparable to ionic liquid based supercapacitors reported in the literature.[22] The EDLS had a large electrochemical window (2.1 V) and the area under the rectangular shape of the CV was larger when compared to ES device CV.[4] As the PPy was bonded through hydrogen bonding to the cellulose matrix, the conductivity was low[11] when compared to a polypyrrole backbone grafted on fabric or cellulose.[23] Therefore the integrated area under the CV for ES device and the electrochemical window (1.6 V) was lower when compared to EDLS (2.1 V) and HS (2.2 V). To enhance electronic conductivity, graphite was added to the PPy-Cell-IL composite matrix and as a result, the CV resulted in a better rectangular shape for the hybrid device.[24] Specific capacitance (C_{Spec}) values were calculated using the integral of the discharge current from the voltammogram and using **Equation 1.** Variation of specific

capacitance values at different scan rates for EDLS, ES and HS are provided in Figure S2, S6 and S10 respectively in the SI. The EDLS device showed the highest specific capacitance (25.8 mF g^{-1}) at the scan rate of 20 mV sec^{-1}, however, the HS had larger working potential (2.2 V). The cycle life of these devices was tested using cyclic voltammetry using a scan rate of 50 mV sec^{-1} (refer Figure S3, S7 and S11 in the SI for voltammograms) upto 15000 cycles. Due to low electronic conductivity of these inherently hydrogen bonded cellulose-polypyrrole composites (ranging between 50 to 5000 μS cm^{-1}), their specific capacitance were low when compared to conducting polymer-grafted systems, however after 15000 cycles these devices retained almost 100% of specific capacitance (see Figure 2b), whereas the polypyrrole coated paper supercapacitor showed 25.4% loss in specific capacitance after 10000 cycles.[25] Most other conducting polymer based supercapacitors decline by 25% in specific capacitance after 5000 cycles.[7b] Pristine graphene oxide based supercapacitors were reported for excellent durability in the literature,[26] however when functionalised with sulfur,[27] the cycle life was drastically reduced. Our supercapacitors with cellulose bonded polypyrrole composite electrodes showed superior durability when compared to systems with polypyrrole deposited on conductive materials such as carbon shell electrodes[28] and hierarchical structures of functionalised graphene with metal oxide based systems.[29]

$$C_{Spec} = \frac{1}{m \cdot \nu \cdot (V_f - V_i)} \int_{V_i}^{V_f} I(V)\,dV \qquad (1)$$

Where m (g) is the mass of the active material in one electrode, ν (V sec^{-1}) is the scan rate, $V_f - V_i$ (V) corresponds to the potential window and $\int_{V_i}^{V_f} I(V)\,dV$ refers to the integral of the discharge current in the voltammogram.

Rate capability determination using constant current galvanostatic charge-discharge studies is another important metric to evaluate supercapacitors. Figure 2c shows the galvanostatic charge-discharge curves of EDLS, ES and HS devices at the current density of 0.05 μA cm^{-2}.

All three types of supercapacitors from this work were subjected to current densities ranging from 0.02 μA cm-2 to 1 μA cm^{-2} to study their charge-discharge capability and equivalent circuit resistance within the working potential range obtained from the cyclic voltammetry (charge-discharge curves for all current densities provided in SI, Figure S4, S8 and S12).

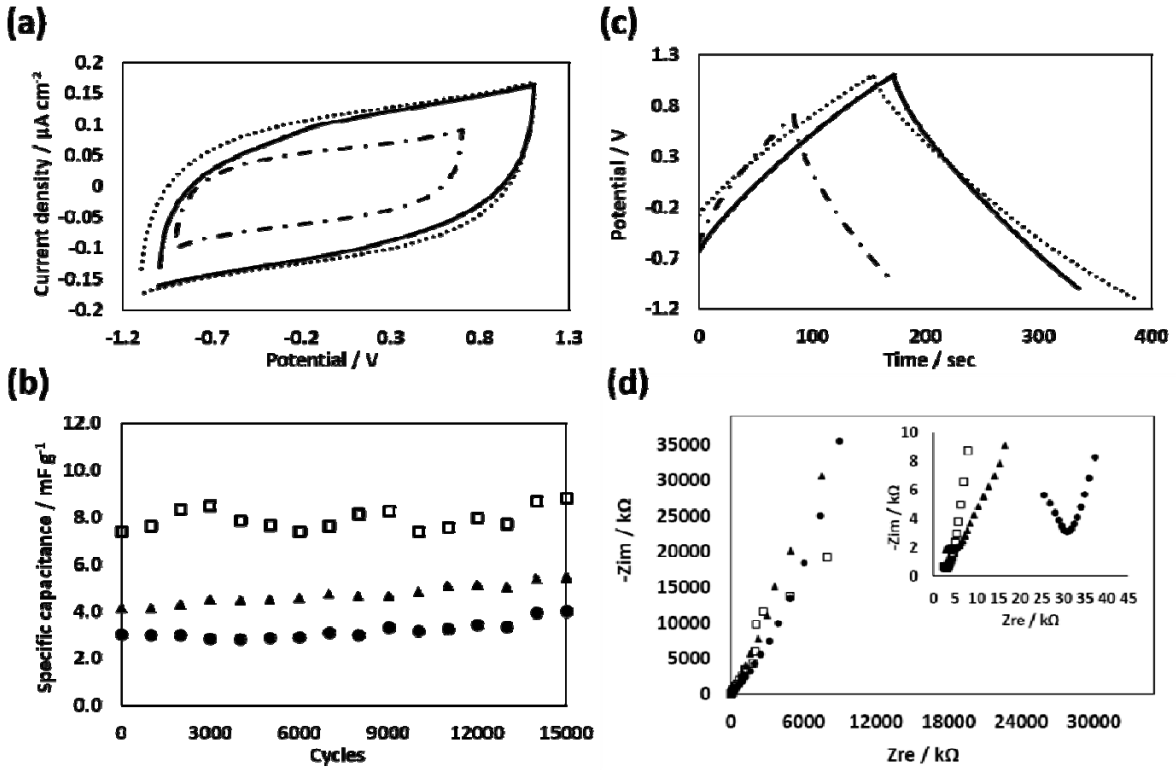

Figure 2. (a) Cyclic voltammograms of — ELDS, ▪▪▪▪▪ HS and — ▪ — ▪ — ES at 50 mV sec^{-1} at 25 °C; (b) specific capacitance values calculated using cyclic voltammograms at scan rate of 50 mV sec^{-1} for □ EDLS, ▲ HS and ● ES; (c) galvanostatic charge-discharge curves at a current density of 0.05 μA cm^{-2} for — ELDS, ▪▪▪▪▪ HS and — ▪ — ▪ — ES at 25 °C; (d) Nyquist plots of □ EDLS, ▲ HS and ● ES after 15000 cycles at 25 °C. Inset: an enlarged scale at high frequency.

The HS showed superior performance than EDLS and ES with longest discharge times, further confirming the reinforcement of electrical properties from graphite and redox properties from PPy. The GCD curves were nearly symmetrical triangles and a small voltage

drop at the commencement of the discharge curves indicated low internal resistance in all these devices, although the resistance of the composite electrode materials was generally high as discussed above. The slow voltage loss with respect to discharge time for the EDLS and HS device showed lower internal resistance of Graphite-Cell-IL and PPy-Cell-IL-graphite composite films when compared to PPy-Cell-IL films. The charge-discharge time for HS of ~400 sec at the current density of 0.05 μA cm^{-2} is comparable to graphene reinforced polyaniline based supercapacitors.[30] Equivalent series resistance (ESR) was calculated using **Equation 2**. ESR values of all devices are provided in **Table 1**.

$$ESR = \frac{IR_{drop}}{I_{const.}} \quad (2)$$

Where IR_{drop} (V) is the internal resistance of the device and $I_{const.}$ (A) corresponds to the current density applied.

Another significant property that can be obtained from the GCD curve is the time required for the device to charge and discharge. The ES (with PPy-Cell-IL as electrodes) was the fastest supercapacitor at all current densities applied, due to the redox mechanism by the polypyrrole backbone in alignment with literature.[4] Electrical impedance spectroscopy (EIS) was used to investigate the ion transport behavior and electrical resistance of the devices developed in this work. Nyquist plots of EDLS, ES and HS devices is presented in Figure 2d after 15000 cycles. In the low frequency region, all the three supercapacitors viz. electrochemical, electrical double-layer and hybrid device show nearly vertical straight lines (~70°) indicating capacitive behaviour and in the medium frequency region the curved line with a slope of about 45° represents Warburg resistance caused by diffusion of electrolyte ions through the porous electrode.

The projected length of the Warburg on the real axis represents ion penetration process.[31] The Warburg length of all devices from this work was shorter when compared to literature,

moreover, EDLS and HS lengths were shorter than the ES device, as the ion diffusion path (charge transfer resistance was smaller) was shorter possibly favored by amorphous cellulose matrix acting as an electrolyte reservoir.[32] Additionally the ionic liquid with a common ion i.e. $[P_{6,6,6,14}][NTf_2]$ as the one present in the electrolyte ($[C_2mim][NTf_2]$) is integrated into the composite electrodes during preparation, ion diffusion from the electrolyte to the electrode is expected to be favoured through the micropockets filled with electrolytes distributed in the cellulose matrix. The component that divides the high-frequency and low-frequency regions on the Nyquist plot is called the knee frequency[33] which is the maximum frequency where the capacitive behavior is maintained. The knee frequency for the devices was in the order of EDLS>HS>ES. The electrochemical properties obtained from cyclic voltammetry, galvanostatic charge-discharge and electrical impedance spectroscopy are tabulated in Table 1.

Table 1. Electrochemical properties obtained from cyclic voltammetry, galvanostatic charge-discharge and electrical impedance spectroscopy for various supercapacitors tested in this work at a temperature of 25 °C.

Techniques	Electrochemical Properties	EDLS	ES	HS
CV	Electrochemical Window [V]	2.1	1.6	2.2
	C_{Spec} at 50 mV sec^{-1} [mF g^{-1}]	7.9	2.8	4.1
	Cycle life at 50 mV sec^{-1} [cycles]	15000	15000	15000
GCD	ESR [kΩ]	168	417	295
	Maximum charge-discharge time at 0.02 μA cm^{-2} [sec]	556	388	1044
	Minimum charge-discharge time at 1 μA cm^{-2} [sec]	8	3	7
	Energy density at 1 μA cm^{-2} [μWh cm^{-2}]	0.002	0.70	0.002
	Power density at 1 μA cm^{-2} [μW cm^{-2}]	2.10	1.60	2.20
EIS	Knee frequency [Hz]	15275	7194	10471

2.2. Chemical and physical characterization

Scanning electron microscopy (SEM) images and infra-red spectra of Graphite-Cell-IL, PPy-Cell-IL and PPy-Cell-IL-Graphite composite films as fresh and after 15000 cycles are presented in **Figure 3**. The fresh Graphite-Cell-IL film (Figure 3a) showed graphite particles embedded within the cellulose matrix and after cycling, a rough surface wherein the graphite particles were more prominent on the surface of the film (Figure 3b) was observed. However, the overall morphology remained the same. This was expected as there was no chemical change during the charge-discharge cycles and the energy device performed due to the electrical double-layer formation which involves the surface activation of graphite particles. The PPy-Cell-IL showed cauliflower looking polypyrrole structures integrated homogenously within cellulose matrix (Figure 3c) as observed earlier.[11] After 15000 cycles, and even after several times of washing with methanol, it was impossible to completely remove the 1-ethyl-3-methylimidazolium bis{(trifluoromethyl) sulfonyl}amide electrolyte. However, it was possible to observe the polypyrrole structures slightly piercing out from the cellulose matrix after long cycling period (Figure 3d). This may be attributed to the breaking of hydrogen bonding between polypyrrole and cellulose competing with the electrochemical reaction happening on the polypyrrole backbone.

Moreover, the volume change[34] occurring during the redox mechanism[35] of conducting polymers is expected to influence the polypyrrole backbone to move outwards to the surface of the cellulose matrix. SEM image of PPy-Cell-IL-Graphite composite film after cycling showed a hybridized structure featuring both Graphite-Cell-IL and PPy-Cell-IL composite films (Figure 3e and f). The SEM images of the other electrode of devices EDLS, ES and HS (Figure S13) and the elemental composition of fresh Graphite-Cell-IL, PPy-Cell-IL and PPy-Cell-IL-Graphite composite films by energy dispersive spectroscopy (Figure S14) is shown in SI.

Infra-red spectra of fresh Graphite-Cell-IL (Figure 3g) shows the characteristic peaks of amorphous cellulose films and $[P_{6,6,6,14}][NTf_2]$ ionic liquid plasticizer as reported in the literature[11] and the large background may be accounted to the black graphite absorbing the infra-red rays. After 15000 cycles, the characteristic vibrations from cellulose and $[P_{6,6,6,14}][NTf_2]$ ionic liquid plasticizer were masked by the graphite dominating the surface of the film, thereby reducing the peak intensities. For PPy-Cell-IL (Figure 3h), after long cycling, the N-H stretching broad peak around 3435 cm^{-1} from polypyrrole became more predominant (resembling the spectra of polypyrrole powder) which is in agreement with the SEM results that the polypyrrole backbone moved to the surface of the film after cycling.

PPy-Cell-IL-Graphite composite films showed no obvious change in the IR spectra of the fresh material compared to the one after 15000 cycles (Figure 3i). This chemical stability observed for HS device after cycling was in agreement with the wider electrochemical window and stable CVs throughout cycling. These homogeneous cellulose-based composite films integrated with ionic liquid showed generally higher stability compared to conducting polymers grafted on paper. Grafting involves the synthesis of conducting polymer on flexible substrates such as paper, fabric or graphene[7-9, 28] creating heterogeneous materials and due to poor adherence to the substrate, supercapacitors based on these materials show capacitance fade after ~5000 cycles.

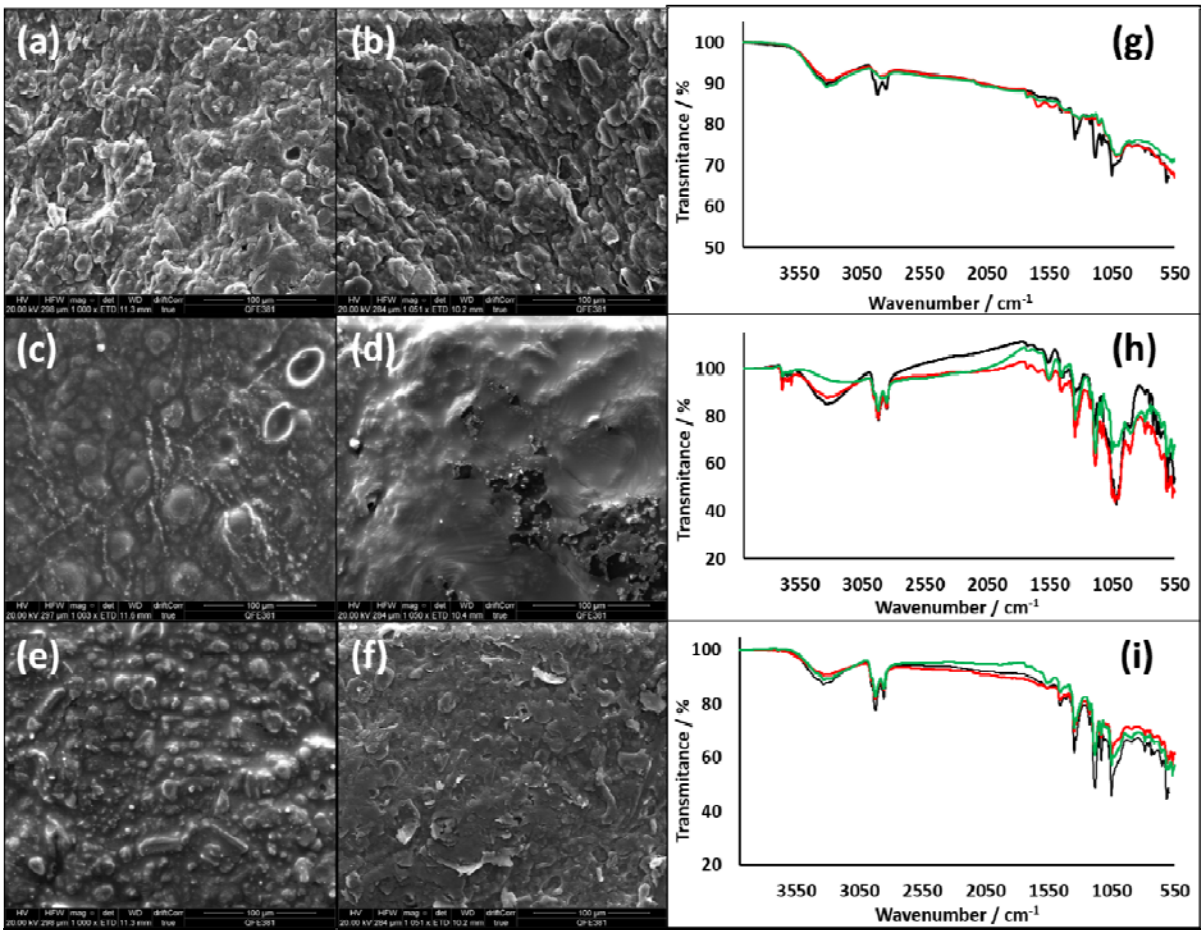

Figure 3. (a), (c) and (e) shows SEM images of fresh Graphite-Cell-IL, PPy-Cell-IL and PPy-Cell-IL-Graphite composite films respectively; (b), (d) and (f) shows SEM images of Graphite-Cell-IL, PPy-Cell-IL and PPy-Cell-IL-Graphite composite films after used as one of the electrodes in the supercapacitors, respectively; (g), (h) and (i) corresponds to infra-red spectra of Graphite-Cell-IL, PPy-Cell-IL and PPy-Cell-IL-Graphite composite films as fresh (black line) and after 15000 cycles for both electrodes (red and green lines).

2.3. Thermal studies and flexibility check

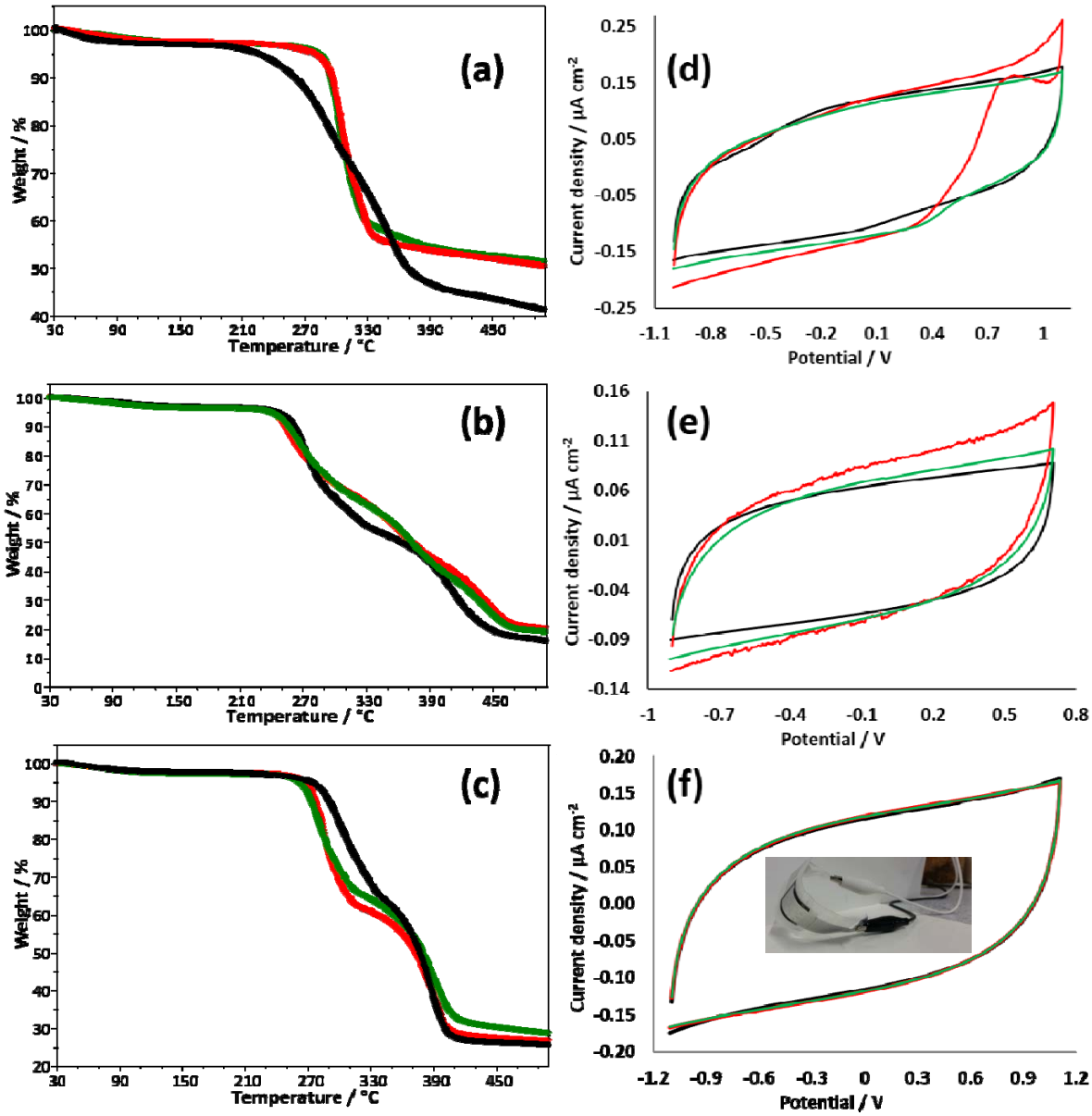

Figure 4. (a), (b) and (c) shows thermogram curves for Graphite-Cell-IL, PPy-Cell-IL and PPy-Cell-IL-Graphite composite films, respectively. The curves correspond to the fresh composite film (black line) and the composite films after 15000 cycles as the two electrodes in the supercapacitors (green and red lines); (d), (e) and (f) shows the bending study of EDLS, ES and HS, respectively. The voltammetry experiment was carried out at the scan rate of 50 mV sec^{-1} and at 25 °C. Before bending (black line), during bending (red line) and after bending (green line).

Thermal degradation of these new composite materials is shown by thermograms in **Figure 4**. An initial weight loss of ~2% until 120 °C may be accounted for the loss of free and bonded water in all three cellulose-based composite films. The onset of thermal degradation in fresh Graphite-Cell-IL film (Figure 4a) occurred at 258 °C and this can be accounted to the amorphous cellulose degradation.[16] Whereas after 15000 cycles, the thermal stability of the composite improved and the onset of degradation temperature shifted to 292 °C. This may be accounted to graphite dispersing homogeneously throughout the cellulose matrix due to electroactivation during the cycling process and stabilized by electrostatic forces of the ionic liquid.[36] The second decomposition around 335 °C may be accounted to the $[P_{6,6,6,14}][NTf_2]$ IL degradation in the fresh Graphite-Cell-IL film. However, this degradation was missing and the residue was higher in the Graphite-Cell-IL films after cycling which may be also accounted for the stabilization effect of ionic liquids on the composite. For PPy-Cell-IL films (Figure 4b) the onset of degradation temperature was at 256 °C and this aligned with the data reported in the earlier literature.[11] The second degradation around 387 °C was expected to be degradation of the conducting polymer (PPy) backbone.

After cycling, as observed in the SEM and IR spectra, the disruption of hydrogen bonding between polypyrrole (-NH) and cellulose (-OH), led to lowering of onset of degradation temperature by ~10 °C and the second degradation was also lowered by ~30 °C. The third decomposition was also observed around 425 °C which may be accounted to the decomposition of the dopant, benzene sulfonate incorporated for charge balance in the polypyrrole-cellulose matrix. It is evident that PPy and cellulose were connected by hydrogen bonding prior to cycling and represented a homogenous material. PPy-Cell-IL-Graphite (Figure 4c) showed two thermal degradations before cycling and after cycling the decomposition temperatures were slightly lowered, overall the film was thermally more stable than Graphite-Cell-IL and PPy-Cell-IL films. Further thermal analysis using static

thermal gravimetric analysis coupled with mass spectrometry using slower scan rates are currently under progress to evaluate the thermal event more precisely in these composites.

Performance test of these energy devices before, during and after bending conditions – 'flexibility check' was determined by cyclic voltammetry. In Figure 4d, the cyclic voltammograms of the ELDS are shown wherein the voltammogram changed in shape and area under CV during and after bending the device. There was a slight distortion observed in the discharge cycle which may be accounted to an electrical disconnection between graphite particles in the cellulose matrix during bending action. In the case of ES, the CVs looked all different (Figure 4e) showing variability in the device performance when bend (resistor behavior), however no distortion in voltammogram shape was observed. This may be accounted to the homogenous nature of the composite material. For HS (Figure 4f) the voltammograms were identical in all situations, demonstrating the stability of this device under bending conditions.

In summary, flexible supercapacitors using novel conducting polymer-cellulose-ionic liquid based composite electrodes that are inherently stable due to hydrogen bonding were fabricated. Graphite-cellulose-ionic liquid composite films were also tested for electrical double-layer capacitance. Three types of devices viz. electrical double-layer supercapacitor, electrochemical supercapacitor and hybrid supercapacitors were constructed and their electrochemical properties were tested using cyclic voltammetry, galvanostatic charge-discharge studies, and electrical impedance spectroscopy. These devices showed excellent stability in device performance with a cycle life of 15000 cycles with almost 100% specific capacitance retained. The chemical nature, morphology and thermal stability of these conducting polymer-cellulose-ionic liquid based electrodes were investigated by infra-red spectroscopy, scanning electron microscopy and thermal gravimetric analysis as fresh materials and after 15000 cycles in order to understand the device functional characteristics.

Chemical stabilization was favored by hydrogen bonding and electrostatic forces in these materials that resulted in higher device stability and flexibility. The hybrid supercapacitor based on polypyrrole-cellulose-ionic liquid-graphite composite as electrode materials showed higher capacitance per geometric area of ~0.05 mF cm^{-2}, the power density of 2.2 μW cm^{-2} and higher chemical, physical and thermal stability after 15000 cycles. This power density is expected to be sufficient to power biosensors in medical implants.[37] Noteworthy, these devices were fabricated using cellulose-based flexible electrodes that were prepared by simple one-pot synthesis using an ionic liquid technology, demonstrating the possibility of recycling biowaste and also assembled using conventional cheap materials for creating a cost-effective system. Moreover, the chemical components used were chosen to be biocompatible and therefore suitable for medical device applications. The bench-top testing demonstrated that these devices are stable to ambient conditions without the requirement for sophisticated sealing and the hydrophobic nature of the composites are favorable for in vivo applications, unlike the paper-based supercapacitors that can disintegrate in aqueous systems. It is expected that the designer nature of various components in these devices will enable to fabricate task-specific supercapacitors with required capacitance and stability to adapt various equipment needs in future. Currently, mechanical properties and biocompatibility studies of these conducting polymer-cellulose-ionic liquid composite materials are in progress in our laboratory.

3. Experimental Section

Preparation of flexible electrodes: Pyrrole (98%) (sealed and stored in the refrigerator), ammonium persulfate (98%), fibrous cellulose long (CAS 9004-34-6) and benzenesulfonic acid (97%) were supplied by Sigma-Aldrich and used without further purification. Ionic liquids (ILs), 1-butyl-3-methylimidazolium chloride ([C_4mim]Cl), trihexyl(tetradecyl)phosphonium bis{(trifluoromethyl)sulfonyl}amide ([$P_{6,6,6,14}$][NTf_2]), and

1-ethyl-3-methylimidazolium bis{(trifluoromethyl)sulfonyl}amide ([C_2mim][NTf_2]) were synthesized at QUILL. All ILs were chemically pure by NMR and had <100 ppm of water determined by Karl Fischer titration.

In a 100 mL round bottom flask equipped with a mechanical stirrer, 3.235 g of [C_4mim]Cl was added and heated under nitrogen at 100 ºC until it was melted and mobile. 10% fibrous cellulose was added, stirred and heating continued at 100 ºC for 3 hours as was described by Swatloski et al. in 2002.[16] 10 wt% [$P_{6,6,6,14}$][NTf_2] IL plasticizer (0.355 g, 0.05 mmol) was added to the mixture. The mixture was stirred until it became homogeneous. Graphite-Cell-IL was prepared by adding 10 wt% graphite (0.358 g) to the cellulose-IL mixture obtained previously and stirred until a homogeneous mixture was obtained. In the case of PPy-Cell-IL, the cellulose-IL mixture was cooled to room temperature, the oxidant, ammonium persulfate (0.113 g, 0.50 mmol) and dopant, benzenesulfonic acid (0.211 g, 1.33 mmol) were added. The dopant quantity was 0.3 mol relative to pyrrole. The mixture was stirred until homogeneity and then, 10 wt% of pyrrole (0.37 mL, 5.00 mmol) was added and stirred further. The PPy-Cell-IL-Graphite composite preparation was prepared similarly to PPy-Cell-IL synthesis followed by adding 10 wt% graphite (0.3938 g) to the mixture and stirred until a homogeneous mixture was obtained.

Cellulose, pyrrole, [$P_{6,6,6,14}$][NTf_2] IL, and graphite were added as 10% by weight of the [C_4mim]Cl IL as solvent. When all the components were dissolved in [C_4mim]Cl, the mixture was cast into a film between two proofing papers and using the bar No. 8 (wet film thickness 100 μm) in a coating machine (K control coater model 101 from RK Printcoat Instruments). Afterward, the wet film cast was immersed into a water bath (antisolvent) to regenerate the cellulose by removing the [C_4mim]Cl IL. After being washed several times with water, the film formed was dried at room temperature in air for 24 hours.

Characterization of flexible electrodes: Solid-state characterization was carried out with a Fourier transform infrared (FTIR) spectrometer (Spectrum 100 from PerkinElmer) equipped with an attenuated total reflectance (ATR) accessory in the range of 4000 - 550 cm^{-1} by accumulating 16 scans at a resolution of 4 cm^{-1}. Thermogravimetric analysis (TGA) was used to determine the thermal stability of the films using a thermogravimetric analyzer Q5000 V3.17 build 265 from TA instruments. Experiments were carried out with a heating rate of 10 °C min^{-1} ranging from 30 to 500 °C under dinitrogen flow at 25 mL min^{-1}. A platinum pan was used as the sample holder. Topography and morphology characteristics were studied using a FEI Quanta FEG Scanning Electron Microscopy (SEM) attached with Energy Dispersive X-ray (EDX) spectrometer from Oxford Instruments and Everhart-Thornley Detector (ETD). The films were sputtered with gold prior to the examination.

Assembly of flexible supercapacitors: The three different films viz. PPy-Cell-IL (33.3 wt% active material in 45.4 mg), Graphite-Cell-IL (33.3 wt% in 27.7 mg) and PPy-Cell-IL-Graphite (50 wt% in 39.7 mg) composite films (active were used as both electrodes (positive and negative electrodes) to construct the flexible supercapacitors viz. electrochemical supercapacitor, electrical double-layer supercapacitor and hybrid supercapacitor respectively, each consisting of a sandwich type assembly with [C_2mim][NTf_2] IL dip coated on a paper sheet (lab tissue paper WW 18 14E, white 2 PLY; thickness: 10 µm) used as a separator and electrolyte. A waterproof polyester self-adhesive film (from Labelplanet) was used for packaging and, kitchen aluminum foil was used as current collectors. All the composite films used as electrodes were dried, prior to assembly, in a vacuum desiccator for 48 hours.

Electrochemical characterization flexible supercapacitors: Potentiostat/Galvanostat Autolab PGSTAT302N from Eco Chemie with GPES software was used to conduct the cyclic voltammetry (CV) and galvanostatic charge-discharge (GCD). CV studies (potentiostat mode), GCD studies (galvanostat mode) were performed using the two electrode flexible

supercapacitors fabricated. The same instrument was used for electrical impedance spectroscopy (EIS) measurements with a built-in frequency response analyzer (FRA). The frequency was logarithmically swept from 100 kHz to 10 mHz with an AC perturbation of 10 mV at open circuit potential. All the electrochemical characterization was carried out at room temperature (25 °C ± 2 °C). Three sets of each device (EDLS, ES and HS) were fabricated identically and tested to confirm reproducibility.

Supporting Information

Supporting Information is available from the Wiley Online Library or from the author.

Acknowledgements

The authors gratefully thank the support of QUILL-Industrial advisory board for PhD studentship to Marta Lorenzo, useful research discussions with Prof Kenneth Seddon (QUILL), Dr Cristina Lagunas (QUILL), Dr Henry Wilson (Merck, Germany) and Dr Peter Klusener (Shell, Netherlands) during the course of the research work.

Received: ((will be filled in by the editorial staff))

Revised: ((will be filled in by the editorial staff))

Published online: ((will be filled in by the editorial staff))

References

[1] M. R. Store, *Smart Materials Applications - Global Market Outlook (2015-2022)*, **2016**, http://www.marketresearchstore.com/report/smart-materials-applications-global-market-outlook-46838, accessed October, 2016

[2] U. S. E. P. Agency, *United States Environmental Protection Agency, Advancing Sustainable Materials Management: Facts and Figures*, **2014**, https://www.epa.gov/smm/advancing-sustainable-materials-management-facts-and-figures, accessed October, 2016

[3] B. E. Conway, *J. Electrochem. Soc.* **1991**, *138*, 1539-1548.

[4] C. Zhong, Y. Deng, W. Hu, J. Qiao, L. Zhang, J. Zhang, *Chem. Soc. Rev.* **2015**, *44*, 7484-7539.

[5] X. Zhang, Z. Lin, B. Chen, S. Sharma, C.-p. Wong, W. Zhang, Y. Deng, *J. Mater. Chem. A* **2013**, *1*, 5835-5839.

[6] H. Shirakawa, E. J. Louis, A. G. Macdiarmid, C. K. Chiang, A. J. Heeger, *J. Chem. Soc., Chem. Commun.* **1977**, 578-580.

[7] a) G. A. Snook, P. Kao, A. S. Best, *J. Power Sources* **2011**, *196*, 1-12; b) I. Shown, A. Ganguly, L.-C. Chen, K.-H. Chen, *Energy Sci. Eng.* **2015**, *3*, 2-26.

[8] J. Chen, J. Xu, K. Wang, X. Qian, R. Sun, *ACS Appl. Mater. Interfaces* **2015**, *7*, 15641-15648.

[9] I. S. Romero, M. L. Schurr, J. V. Lally, M. Z. Kotlik, A. R. Murphy, *ACS Appl. Mater. Interfaces* **2013**, *5*, 553-564.

[10] J. Kim, S. D. Deshpande, S. Yun, Q. Li, *Polym. J.* **2006**, *38*, 659-668.

[11] M. Lorenzo, B. Zhu, G. Srinivasan, *Green Chem.* **2016**, *18*, 3513-3517.

[12] M. Armand, F. Endres, D. R. MacFarlane, H. Ohno, B. Scrosati, *Nat. Mater.* **2009**, *8*, 621-629.

[13] A. Kim, M. Ochoa, R. Rahimi, B. Ziaie, *IEEE Access* **2015**, *3*, 89-98.

[14] H. G. Mond, G. Freitag, *Pacing and Clinical Electrophysiology* **2014**, *37*, 1728-1745.

[15] D. C. Bock, A. C. Marschilok, K. J. Takeuchi, E. S. Takeuchi, *Electrochim. Acta* **2012**, *84*, 155-164.

[16] R. P. Swatloski, S. K. Spear, J. D. Holbrey, R. D. Rogers, *J. Am. Chem. Soc.* **2002**, *124*, 4974-4975.

[17] a) M. P. Scott, M. Rahman, C. S. Brazel, *Eur. Polym. J.* **2003**, *39*, 1947-1953; b) M. Rahman, C. S. Brazel, *Polym. Degrad. Stab.* **2006**, *91*, 3371-3382.

[18] A. M. A. Dias, S. Marceneiro, M. E. M. Braga, J. F. J. Coelho, A. G. M. Ferreira, P. N. Simões, H. I. M. Veiga, L. C. Tomé, I. M. Marrucho, J. M. S. S. Esperança, A. A. Matias, C. M. M. Duarte, L. P. N. Rebelo, H. C. de Sousa, *Acta Biomaterialia* **2012**, *8*, 1366-1379.

[19] X. Jia, C. Wang, V. Ranganathan, B. Napier, C. Yu, Y. Chao, M. Forsyth, F. G. Omenetto, D. R. MacFarlane, G. G. Wallace, *ACS Energy Lett.* **2017**, *2*, 831-836.

[20] E. Frackowiak, F. Beguin, *Carbon* **2001**, *39*, 937-950.

[21] J. H. Park, O. O. Park, K. H. Shin, C. S. Jin, J. H. Kim, *Electrochem. Solid State Lett.* **2002**, *5*, H7-H10.

[22] a) M. M. Perez-Madrigal, M. G. Edo, C. Aleman, *Green Chem.* **2016**, *18*, 5930-5956; b) A. Lewandowski, M. Galiński, *J. Phys. Chem. Solids* **2004**, *65*, 281-286; c) G. P. Pandey, A. C. Rastogi, *J. Electrochem. Soc.* **2012**, *159*, A1664-A1671.

[23] J. Xu, D. Wang, Y. Yuan, W. Wei, S. Gu, R. Liu, X. Wang, L. Liu, W. Xu, *Cellulose* **2015**, *22*, 1355-1363.

[24] J. Chmiola, C. Largeot, P.-L. Taberna, P. Simon, Y. Gogotsi, *Science* **2010**, *328*, 480.

[25] L.-L. Xu, M.-X. Guo, S. Liu, S.-W. Bian, *RSC Adv.* **2015**, *5*, 25244-25249.

[26] S.-K. Kim, H. J. Kim, J.-C. Lee, P. V. Braun, H. S. Park, *ACS Nano* **2015**, *9*, 8569-8577.

[27] X. Yu, H. S. Park, *Carbon* **2014**, *77*, 59-65.

[28] T. Liu, L. Finn, M. Yu, H. Wang, T. Zhai, X. Lu, Y. Tong, Y. Li, *Nano Lett.* **2014**, *14*, 2522-2527.

[29] B. G. Choi, Y. S. Huh, W. H. Hong, D. Erickson, H. S. Park, *Nanoscale* **2013**, *5*, 3976-3981.

[30] P. Yu, X. Zhao, Z. Huang, Y. Li, Q. Zhang, *J. Mater. Chem. A* **2014**, *2*, 14413-14420.

[31] W. J. Albery, Z. Chen, B. R. Horrocks, A. R. Mount, P. J. Wilson, D. Bloor, A. T. Monkman, C. M. Elliott, *Faraday Discuss. Chem. Soc.* **1989**, *88*, 247-259.

[32] D.-W. Wang, F. Li, M. Liu, G. Q. Lu, H.-M. Cheng, *Angew. Chem., Int. Ed.* **2008**, *47*, 373-376.

[33] M. Hughes, G. Z. Chen, M. S. P. Shaffer, D. J. Fray, A. H. Windle, *Chem. Mater.* **2002**, *14*, 1610-1613.

[34] L. Bay, T. Jacobsen, S. Skaarup, K. West, *J. Phys. Chem. B* **2001**, *105*, 8492-8497.

[35] K. Okabayashi, F. Goto, K. Abe, T. Yoshida, *Synth. Met.* **1987**, *18*, 365-370.

[36] J. Dupont, J. D. Scholten, *Chem. Soc. Rev.* **2010**, *39*, 1780-1804.

[37] P. Patel, *Dissolvable batteries made of silk*, **2017**, http://cen.acs.org/articles/95/web/2017/04/Dissolvable-batteries-made-silk.html?+Engineering+News%3A+Latest+News%29, accessed April, 2017

Graphical Abstract for Table of Contents

Durable Flexible Supercapacitors Using Multifunctional Role of Ionic Liquids

M. Lorenzo and G. Srinivasan*

School of Chemistry and Chemical Engineering, The QUILL Research Centre, David Keir Building, Queen's University Belfast, Stranmillis Road Belfast BT9 5AG, UK
g.srinivasan@qub.ac.uk

Keywords: conducting polymers, ionic liquids, supercapacitors, flexible energy devices, medical device

Chemically blended polypyrrole-cellulose composites integrated with ionic liquid shows potential to fabricate task-specific environmentally safer supercapacitors that are durable and flexible to power up next generation electronic equipment and medical implants.

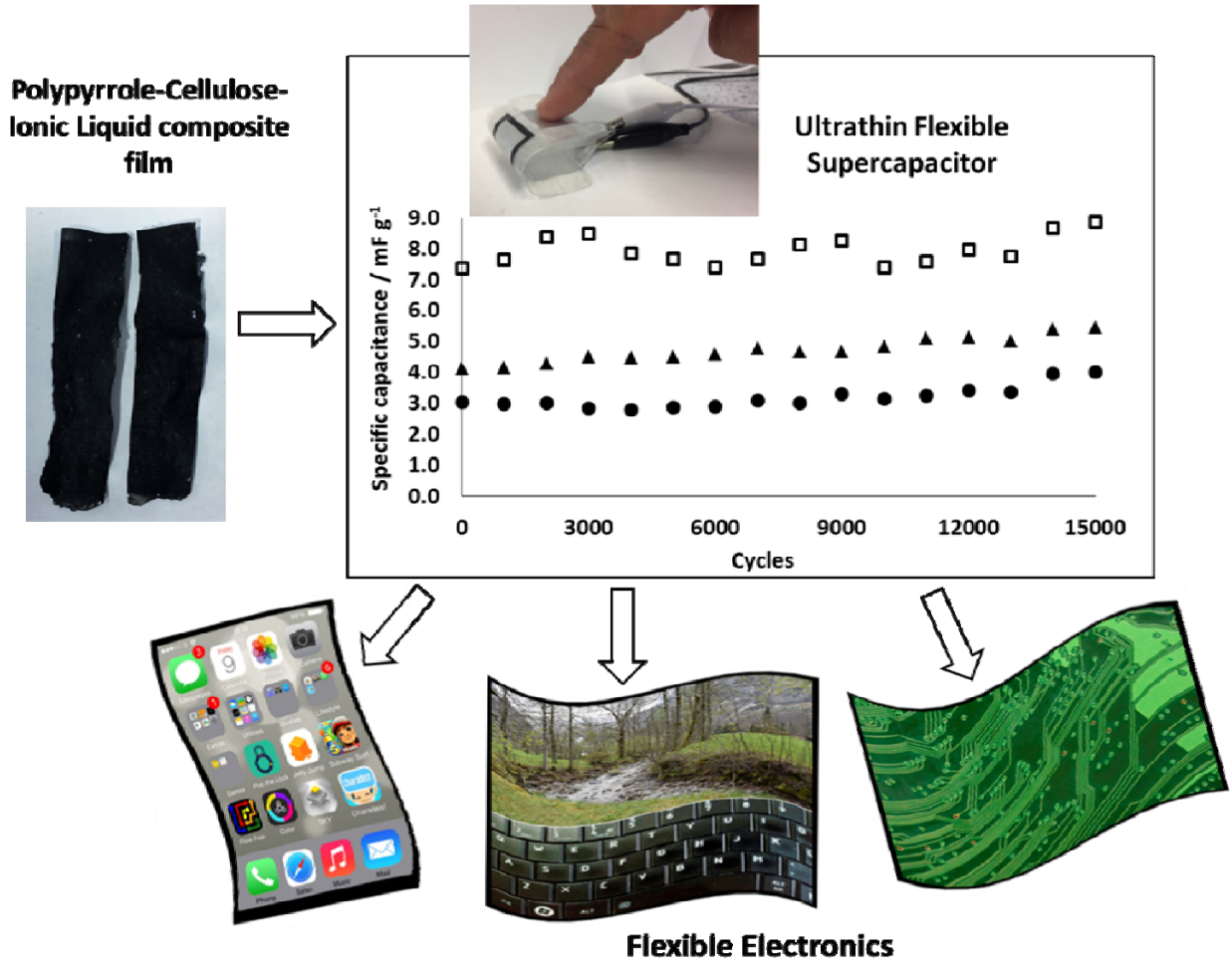

Figure 1. Schematic of the fabrication process of polypyrrole-cellulose-ionic liquid composite films leading to flexible supercapacitors.

Figure 2. (a) Cyclic voltammograms of — EDLS, ▪▪▪▪▪ HS and ─ ▪ ─ ▪ ─ ES at 50 mV sec^{-1} at 25 °C; (b) specific capacitance values calculated using cyclic voltammograms at scan rate of 50 mV sec^{-1} for □ EDLS, ▲ HS and ● ES; (c) galvanostatic charge-discharge curves at a current density of 0.05 μA cm^{-2} for — EDLS, ▪▪▪▪▪ HS and ─ ▪ ─ ▪ ─ ES at 25 °C; (d) Nyquist plots of □ EDLS, ▲ HS and ● ES after 15000 cycles at 25 °C. Inset: an enlarged scale at high frequency.

Figure 3. (a), (c) and (e) shows SEM images of fresh Graphite-Cell-IL, PPy-Cell-IL and PPy-Cell-IL-Graphite composite films respectively; (b), (d) and (f) shows SEM images of Graphite-Cell-IL, PPy-Cell-IL and PPy-Cell-IL-Graphite composite films after used as one of the electrodes in the supercapacitors, respectively; (g), (h) and (i) corresponds to infra-red spectra of Graphite-Cell-IL, PPy-Cell-IL and PPy-Cell-IL-Graphite composite films as fresh (black line) and after 15000 cycles for both electrodes (red and green lines).

Figure 4. (a), (b) and (c) shows thermogram curves for Graphite-Cell-IL, PPy-Cell-IL and PPy-Cell-IL-Graphite composite films, respectively. The curves correspond to the fresh composite film (black line) and the composite films after 15000 cycles as the two electrodes in the supercapacitors (green and red lines); (d), (e) and (f) shows the bending study of EDLS, ES and HS, respectively. The voltammetry experiment was carried out at the scan rate of 50 mV sec^{-1} and at 25 °C. Before bending (black line), during bending (red line) and after bending (green line).

Table 1. Electrochemical properties obtained from cyclic voltammetry, galvanostatic charge-discharge and electrical impedance spectroscopy for various supercapacitors tested in this work at a temperature of 25 °C.